The Design of Amino Hydroxamic Metal Chelates and Their Activity in Biological Systems. Formation Constants between 2-Amino-4-methylpentanehydroxamic Acid with Proton, Copper(II), and Iron(III) in Aqueous Solution

Enrico LEPORATI* and Gianluca NARDI
Istituto di Chimica Generale ed Inorganica, Universita' degli Studi di Parma,
Viale delle Scienze, 78, 43100-PARMA, Italy
(Received November 9, 1990)

The complex-formation equilibria and relative stability constants of species present in aqueous solution of copper(II) and iron(III) with "L-leucinehydroxamic acid" (2-amino-4-methylpentanehydroxamic acid, ahmpe) have heen determined by using potentiometric and spectrophotometric titrations in 0.5 mol dm^{-3} KCl solution at 25 °C. Their acid-base reaction stoicheiometries have heen evaluated and the protonation constants calculated from potentiometric data with the aid of the GAUSS Z and SUPERQUAD programs. The complex formation constants have heen determined by using SQUAD (absorbance data), SUPERQUAD and STBLTY (potentiometric data) programs. The ligand is bound to the metal ions through the coordination of the N atoms of the α-amino group and the deprotonated $-NHO^-$ group in copper(II)–ahmpe system. For iron(III)–ahmpe system the coordination is referred to oxygen atoms of carboxylate and hydroxamate moieties. The UV-visible studies provide important evidence for the formation of several complex species depending on the pH. The experimental curves [$\varepsilon=f(\lambda)$], deduced from refinement of absorbance data with the program SQUAD, have been split up into precisely positioned absorption bands by Gaussian analysis using a nonlinear least-squares computer program NLIN. So the solution electronic spectra have been also employed to estimate the coordination sphere and have let us to suppose a weak tetragonal coordination [$CuL_2(H_2O)_2$] and octahedral for Fe^{3+} complexes. The determination of formation constants and the coordination pattern proposed have a great interest in terms of metal chelate structures and their important role in biological systems.

Several studies have been recently carried out on hydroxamic acids and their metal complexes owing to the possible biological activity connected with these compounds. Some of these have shown to be potent inhibitors of aminopeptidase,[1–3] a zinc metallo-protease, of enzyme 5-Lipoxygenase[4,5] which is associated with a variety of diseases states as asthma and allergy. Besides several peptide–hydroxamic acids have been designed as inhibitors of human skin collagenase[6] (*Z*-Pro–Leu–Gly–NHOH), Enkephalin-Degrading Enzymes[7,8] (Tyr–Gly–Gly–Phe–Leu), Thermolysin[9] and of a Converting Enzyme of Angiotensin I[10] (L-Glu–(NHOH)–L-Pro for example). Because of the interest about peptide–hydroxamic acids, especially tripeptide such as Pro–Leu–Gly–NHOH, recent works[11,12] have pointed out the importance of thermodynamic stabilities of metal transition complexes containing peptide–hydroxamic polydentate ligands. The authors have not found a relationship with the peptide chain indicating there is no significant interaction in solution. A more recent interest in the class of hydroxamic acids has been increasing mainly due to their capabilities of binding Fe^{3+}. The so-called siderophores are iron chelates microbially produced; they can be divided in iron chelates based on hydroxamic moiety and iron chelates based on catechol group, such as Enterobactin.[13] Several tripod-like hydroxamates and dihydroxamic acids have been synthesized[14,15] and, in order to simulate the properties of natural siderophores ferrichrome,[16] tests in vivo have been carried out. In fact an adequate iron supply is necessary to the growth of bacters. Iron is an essential element for almost all living organisms and also in human body (ca. 4 g), but it is very toxic when in excess. The complex Fe^{3+}–glycinehydroxamic acid has been proposed in veterinary terapy against iron anemy and has been proved to react with Apotransferrin, an iron transport protein.[17] Besides certain macrocyclic ligands[18] containing hydroxamate moieties make the reduction potentials Fe(III)/Fe(II) highly negative but also complexes with unusually high oxidation states are stabilized. For example hydroxamic acids form high colored chelates with V(V) or V(IV); these complexes have been employed extensively as analytical reagents for the detection of this metal.[19–21] In the light of potentiometric and spectrophotometric studies some authors[22,23] have discussed the mechanism of complex formation of Fe^{3+}–glycinehydroxamic acid and Ni^{2+}–pyridoxal-glycinehydroxamic acids. Important results have been obtained about the reactive species [$Fe(OH)^{2+}$, $Fe(OH)_2^+$, Ni^{2+}, and $Ni(OH)^+$] implicated in the formation equilibria. It must be emphasized that it's important to investigate the complexing ability of hydroxamic acids not only with iron but also with Cu^{2+}, Zn^{2+}, Ni^{2+}, Mn^{2+}, Co^{2+}, and Cr^{3+}. So the inhibition of urease has been interpreted in terms of reversible binding to the active site nickel ion[24] and other complexes, once considered harmful to organisms, today are regarded necessary in animal nutrition. In continuation of our efforts, potentiometric and spectrophotometric studies have been carried out dealing with transition metal complexes of L-Leucinehydroxamate with iron(III) and copper(II).

Experimental

Reagents. The ligand ahmpe was obtained from Sigma (St. Louis, MO) and its purity was checked through potentiometric titrations. Doubly distilled and deionized water was used in all titrations prepared to have a final volume of 25 cm^3 and thermostatted at 25.0±0.1 °C, with a Paratherm electronic (Julabo) circulating constant temperature water bath. All titrations were carried out under an atmosphere of purified nitrogen. The concentration of stock solution of bivalent metal chloride [$CuCl_2 \cdot 2H_2O$] (AnalaR Products) was determined by using an electrogravimetric method, while standard stock solution for atomic absorption spectrometry has been employed determining iron [$Fe(NO_3)_3$]. The ionic strength was kept at 0.5 mol dm^{-3} with KCl (Merck). Potassium hydroxide (carbonate free) was utilized as titrating solution (0.3840 mol dm^{-3}) and standardized according to Gran's method as previously described.[25,26] Molarity of hydrochloric acid was determined with anhydrous sodium carbonate, using phenolphthalein (solution at 10%) as indicator.

Potentiometric Measurements. Potentiometric titrations were performed using a Metrohm E 636 Titroprocessor and a combined electrode 8102SC ROSS (ORION Research). Quantities of the titrant KOH were added by using a Metrohm Dosimat E 635 autoburet. All titration solutions were prepared with a final volume of 25 cm^3 and kept at constant temperature of 25±0.1 °C. The solution was shaken employing a mechanical stirrer and it was maintained in the vessel a stream of nitrogen presaturated with water vapor, by bubbling over the surface of the solution. The range of concentration of ligand in potentiometric titrations was 0.0077—0.0096 mol dm^{-3} for ahmpe-H^+ (pH range 3.20—11.24; number of titrations 6); 0.0076—0.0082 mol dm^{-3} for ahmpe-Cu^{2+} (pH range 3.02—10.67; number of titrations 6); 0.0104—0.0239 mol dm^{-3} for ahmpe-Fe^{3+} (pH range 1.77—7.58; number of titrations 10). The concentration of metal varied between 0.00164—0.00532 mol dm^{-3} for ahmpe-Cu^{2+} and 0.00153—0.00785 mol dm^{-3} for ahmpe-Fe^{3+} system using as supporting electrolyte potassium chloride (I=0.5 M) (1 M=1 mol dm^{-3}). Periodic titrations (dynamic) of hydrochloric acid were carried out with standard carbonate-free potassium hydroxide solution according to Gran's method.

Spectrophotometric Measurements. Absorption spectra in the ranges 400—820±0.3 nm for Cu^{2+}-ahmpe and 300—700±0.3 nm for Fe^{3+}-ahmpe systems were recorded on Kontron Uvikon 860 spectrophotometer to the fourth decimal place with a stepping of 2 nm. Solution containing ligand and metal ion, prepared and maintained under nitrogen with ionic strength 0.5 mol dm^{-3} (KCl), were analysed at a series of pH from 3.30 to 8.80, using 10 mm cells for Cu^{2+}-ahmpe and from 1.89 to 7.89 pH values using 1 mm cells for Fe^{3+}-ahmpe systems.

Calculations. Great accuracy has been taken in the calculation and critical evaluation of some parameters (E°, A_j, B_j, N, K_w) relative to potentiometric calibration curves, using different mathematical procedures as previously described.[27,28] An initial estimate of complex formation constants was achieved by the program GAUSS Z.[29] In this program the function $\bar{n}$ against pH let us to estimate the stoicheiometries of possible complexes in the case of binary systems. Successively the SUPERQUAD program[30] was employed to refine the formation constants which minimize the sum of squared residual between observed and calculated emf values (Eq. 1):

$$U=\sum_{i=1}^{z} w_i(E_i^{\text{obsd}}-E_i^{\text{calcd}})^2, \quad (1)$$

where z is the total number of potentiometric data and w_i is the weighting factor defined by equation (Eq. 2):

$$w_i=1/[\sigma_{E_i}{}^2+(\partial E_i/\partial v_i)^2\sigma_{v_i}{}^2], \quad (2)$$

where σ_E(=0.2) and σ_v(=0.008) are respectively the error in emf and in the volume used in the refinement. Moreover STBLTY was utilized to refine formation constants (K-forms or β-forms). In this program a recent pH titration method (FICS) has been used to calculate free metal ions and free ligand concentrations from experimental data without any hypothesis about species for the system.[31,32] The calculation of stability constants then can be reduced to a linear least-square problem by using any of the mass balance equations. The subprogram NONLINEAR LS REFINE is the most commonly used refinement program in STBLTY. The final choice between different SUPERQUAD analyses was based on graphical comparisons between calculated curves and the corresponding simulated data obtained from the HALTAFALL[33] computer program. Besides a further confirmation of potentiometric data has been performed on spectrophotometric values by means of program SQUAD,[34] in which formation constants are refined on the basis of comparison between observed and calculated absorbance values. All the calculations were carried out on the CRAY Y-MP8/432 and IBM 4341/10 computers of the Consorzio per la Gestione del Centro di Calcolo Elettronico dell' Italia Nord Orientale, Casalecchio di Reno, Bologna, Italy, with financial support coming from the University of Parma. Listing of experimental data and final computations from SUPERQUAD, GAUSS Z, NBAR, and SQUAD are available on request from the authors.

Results and Discussion

Protonation Equilibria. Starting from the set of potentiometric data, first the overall protonation constants and the initial amounts (mmol) of reagents (T_L, T_H) were refined simultaneously by using SUPERQUAD. In this calculation the liquid junction potentials (A_j, B_j) have been neglected because of their littleness (pH interval 3.20—10.54) as shown in already published papers.[27,28] The variances (σ^2) in the quantities T_L and T_H of this refinement were respectively 5.2137×10^{-7} and 1.353×10^{-6} $mmol^2$. It might be pointed out (Fig. 1) the excellent agreement between observed and calculated pH values as a function of volume of added titrating solution. The trend of these curves also reflects the presence of two distinct buffering zones separated between them by a small inflection point. The first buffer zone in the pH range 6.10—8.45 corresponds to deprotonation of the oxygen atom ($\log K_2^{H}$=7.263); the second zone in the pH range 8.00—10.30 is due to deprotonation of α-amino group ($\log K_1^{H}$=9.152). Besides two titrations have been stopped at pH 7.7 (Fig. 1a) and 8.2 (Fig. 1b) because of the low solubility of ligand in aqueous solution due to its lipophilic character. The cumulative and stepwise protonation and complex formation constants of ahmpe are quoted in

Table 1. Cumulative and Stepwise Protonation Complex Formation of 2-Amino-4-methylpentanehydroxamic Acid (ahmpe) at 25 °C and I=0.5 mol dm^{-3} (KCl)

	SUPERQUAD			GAUSS Z	STBLTY (Nonlinear Ls=pM pL pH DATA)	
	H^+	Cu^{2+}	Fe^{3+}	H^+	H^+	Fe^{3+}
$\log\beta_{011}$	9.152(3)			9.152(2)	9.156(3)	
$\log\beta_{021}$	16.416(4)			16.411(2)	16.417(2)	
$\log K_2^{H}$ [a]	7.263(4) [b]			7.260(2)	7.261(2)	
$\log\beta_{101}$		10.626(50)				
$\log\beta_{102}$		19.202(21)	22.89(9)			22.85(3)
$\log\beta_{1-12}$		9.175(83)	15.98(3)			15.94(2)
$\log\beta_{2-12}$		20.592(19)				
$\log K_2$		8.576(38)				
$\log\beta_{111}$			16.65(2)			16.67(1)
$\log\beta_{112}$			28.50(3)			28.56(1)
$\log\beta_{122}$			32.60(1)			32.61(1)
$\log\beta_{103}$			28.00(9)			28.08(3)
$\log\beta_{2-22}$			21.48(7)			21.45(3)
$\log\beta_{113}$			35.55(5)			35.62(2)
$\log\beta_{123}$			41.93(5)			42.02(2)
$\log\beta_{2-13}$			35.40(9)			35.36(3)
z [c]	230	209	430	230	230	378
U	3.43×10^{1}	1.32×10^{3}	1.19×10^{3}	8.11×10^{-3} [f]	2.75×10^{2}	
χ^2 [d]	2.56	7.0	8.77			
σ [e]	0.3985	2.5373	1.70	3.56×10^{-5} [g]	1.099	0.54/0.46/3.54
R [h]					0.3%	0.3/0.2/1.7%

a) $\log K_n=\log\beta_{0n1}-\log\beta_{0n-11}$. b) $\sigma(\log K_n)=\{[\sigma^2(\log\beta_{0n1})+\sigma^2(\log\beta_{0n-11})/2]\}^{1/2}$. c) Total number of experimental data points used in the refinement. d) Observed χ^2; calculated value (6, 0.95) should be 12.6, where 6 is the number of degrees of freedom and 0.95 is the confidence coefficient in the χ^2 distribution. e) $\sigma=\sqrt{\sum_{i=1}^{z}w_i(E_i^{obsd}-E_i^{calcd})^2/(Z-m)}$ for SUPERQUAD and $\sigma=\sqrt{\sum_{i=1}^{z}w_i(pH_i^{obsd}-pH_i^{calcd})^2/(Z-m)}$ for STBLTY, where m is the number of parameters to be refined. f) $U=\sum_{i=1}^{z}(\bar{n}_i^{calcd}-\bar{n}_i^{obsd})^2$, where $\bar{n}_i$ is the observed (obsd) or calculated (calcd) average number of hydrogen ions bound to each central ligand molecule. g) $\sigma^2=\sum_{i=1}^{z}(\bar{n}_i^{calcd}-\bar{n}_i^{obsd})^2/(Z-m)$. h) $R=\sqrt{\sum_{i=1}^{z}(\bar{n}_i^{obsd}-\bar{n}_i^{calcd})^2/\sum_{i=1}^{z}(\bar{n}_i^{obsd})^2}\times100$ for GAUSS Z and $R=\sqrt{\sum_{i=1}^{z}(pH_i^{obsd}-pH_i^{calcd})^2/\sum_{i=1}^{z}(pH_i^{obsd})^2}\times100$ for STBLTY.

Table 1.

The ligand exhibits two protonation centers: The terminal hydroxamate moiety (H^1; Chart 1) and the α-amino group (H^2; Chart 1). In addition to SUPERQUAD, GAUSS Z and STBLTY programs were employed to refine protonation constants starting from the same experimental data and the results agree closely. Kurzak and collaborators[35] reported values of $\log\beta_{011}$=9.12 and $\log\beta_{021}$=16.26 at 0.1 mol dm^{-3} ($NaClO_4$) at 25 °C. Small differences with our values might be justified (especially for $\log K_2$=7.14) by the influence of the ionic strength on the protonation constants, which we obtain at I=0.5 mol dm^{-3} (KCl). It must be noticed that the presence of the α-amino group in ahmpe increases the acidity of the OH group (-NHOH) in comparison with the corresponding hydroxamic acid $CH_3CH(CH_3)$-CH_2CH_2-CONHOH [$\log K$=9.67(3)[36]]. In the same way the replacement of -NHOH moiety for the OH group lowers considerably the protonation constant of the α-amino group due to the greater electron-withdrawing effect of the -NHOH group.

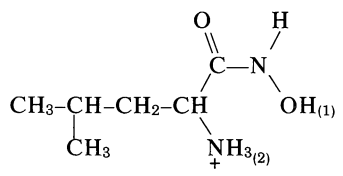

Hahmpe

Chart 1. H_2L^+ with the two removable protons (1 and 2).

Metal Complex Equilibria. Starting from several sets of potentiometric data, obtained in different ligand to metal ratios, many attempts have been carried out to obtain the best fitting chemical models applying SUPERQUAD program, whereas all the protonation constants were kept constant. The refinement included as fixed contributions (very small) the known metal hydrolysis constants[37,38] for the species $[Fe(OH)]^{2+}$, $[Fe(OH)_2]^{+}$, $[Fe_2(OH)_2]^{4+}$, and $[Fe_3(OH)_4]^{5+}$. All the overall formation constants calculated by both computer methods (SUPERQUAD and STBLTY, see Table 1) agreed closely, even though the standard deviations of the refined quantities calculated by SUPERQUAD program were slightly higher. Equilibria between Co^{2+} and Ni^{2+} ions and ahmpe cannot be studied because

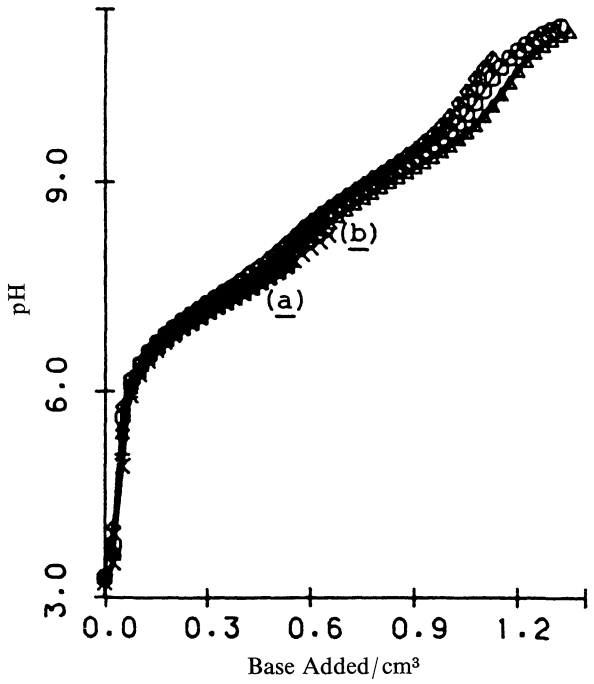

Fig. 1. Experimental and calculated (by SUPERQUAD program) titration curves of pH as a function of volume of KOH added for H^+–ahmpe system, V_o=25 cm³, C_{KOH}=0.38412 mol dm⁻³ [T_L range 0.19365—0.24025, T_H range 0.40614—0.49798]. T_L and T_H are mmol of ahmpe and hydrogen ion in the titration vessel.

precipitation occurs at already acid pH. The refinement converged satisfactorily when only species present for Cu^{2+}–ahmpe system were $[CuL]^+$, $[Cu_2(OH)L_2]^+$, $[CuL_2]$ and $[Cu(OH)L_2]^-$. The most consistent set of complexes found for Fe^{3+}–ahmpe system, together with their respective formation constants shown in Table 1, was $[FeL_2]^+$, $[FeHL]^{3+}$, $[FeH_2L_2]^{3+}$, $[FeHL_2]^{2+}$, $[Fe_2(OH)_2L_2]^{2+}$, $[Fe_2(OH)L_3]^{2+}$, $[FeH_2L_3]^{2+}$, $[FeHL_3]^+$, $[FeL_3]$, and $[Fe(OH)L_2]$. In Fig. 2 species distribution curves are reported. In the case of Cu^{2+}–ahmpe system the complexation begins at pH ca. 3.0 with the formation of $[CuL]^+$ and the dimer $[Cu_2(OH)L_2]^+$ species, which reaches its maximum concentration of 87.0% at pH 4.75. Previous authors[39,40] too have concluded that the dimer is in equilibrium with the mononuclear complex $[CuL]^+$, which is present in small quantity (maximum of 19.99% at pH 3.80). The species $[CuL_2]$ reaches a maximum concentration of 99.8% total copper at pH 7.2 (Fig. 2a)]. Typical absorption spectra for Cu^{2+}–ahmpe are plotted in Fig. 3a, in the pH range 3.75—6.32. At low pH a broad absorption spectrum is present and its maximum shifts towards visible region as the pH increases [maximum, 0.064 A at 724 nm(1); 0.154 A at 654 nm(2); 0.218 A at 644 nm(3); Fig. 3a]. The first maximum of absorbance in the range 586—724 nm occurs at pH 4.66 and λ_{max} of 644 nm and corresponding ca. to the maximum concentration of the hydrolyzed dimeric complex (see Fig. 2a). The increase in absorp-

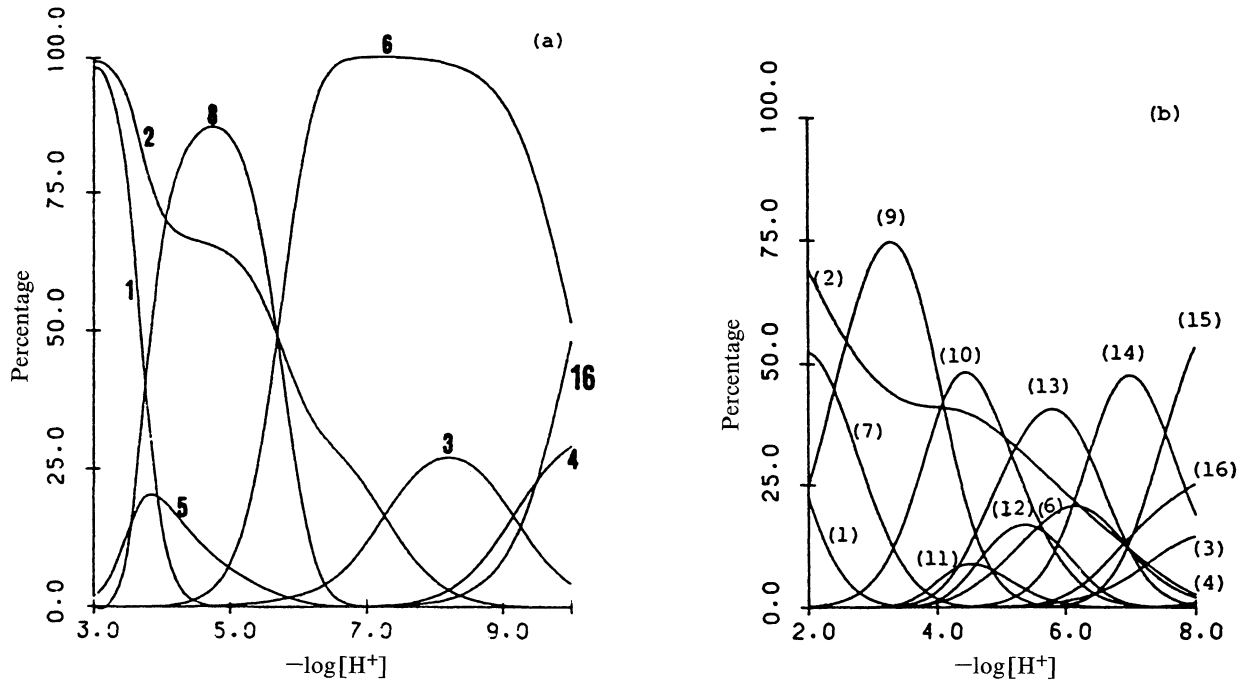

Fig. 2. Typical distribution diagrams for M^{n+}–ahmpe system. The percentage of each species has been calculated from the data of a hypothetical solution of metal ions (0.004 mol dm⁻³ for Cu^{2+} and 0.006 mol dm⁻³ for Fe^{3+}) and ahmpe (0.012 mol dm⁻³ for Cu^{2+} and 0.02 mol dm⁻³ for Fe^{3+}) by the HALTAFALL program (N. Ingri, W. Kakalowicz, L. G. Sillén, and B. Warnqvist, **14**, 1261 (1967)), and using a PLOTTER Calcomp 936. The concentrations of the species not containing metal were calculated as percentages of the total ligand, those containing metal as percentages of the total metal. (a) Cu^{2+}–ahmpe, (b) Fe^{3+}–ahmpe; (1) M^{n+}, (2) H_2L; (3) HL; (4) L; (5) CuL; (6) ML_2; (7) FeHL; (8) $Cu_2(OH)L_2$; (9) FeH_2L_2; (10) $FeHL_2$; (11) $Fe_2(OH)_2L_2$; (12) $Fe_2(OH)L_3$; (13) FeH_2L_3; (14) $FeHL_3$; (15) FeL_3; (16) M $(OH)L_2$.

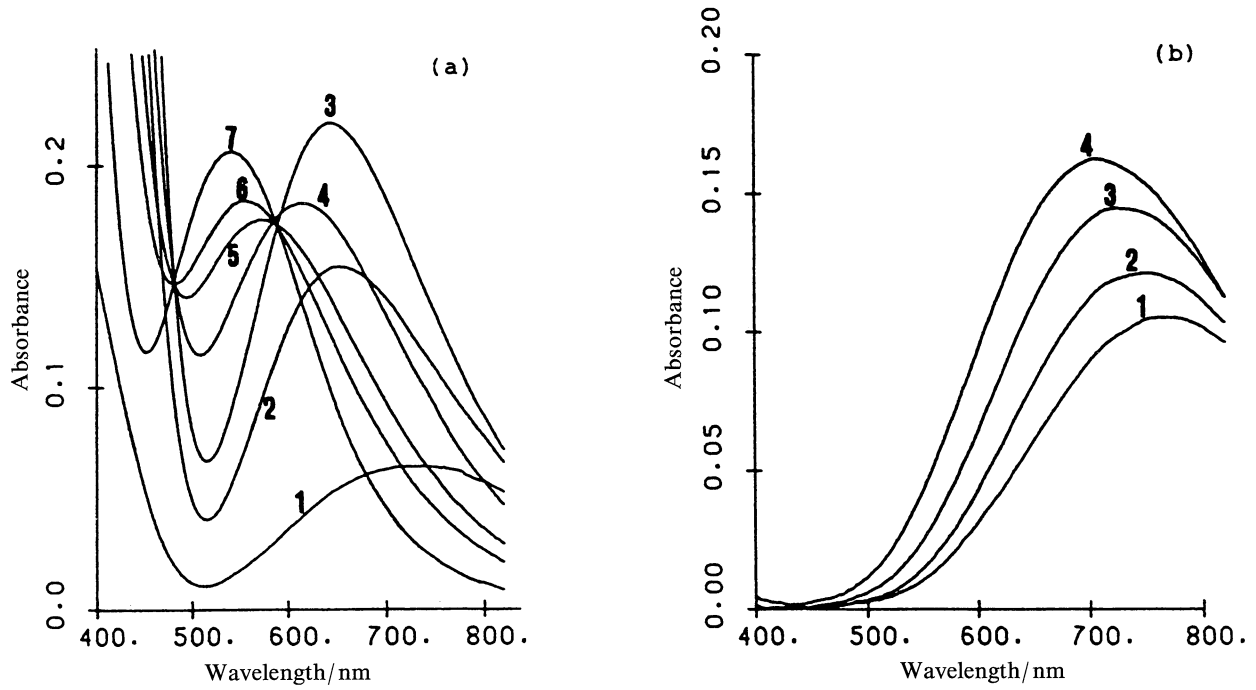

Fig. 3. Plots of experimental absorbance data versus wavelength for solutions [(a), C_L range 7.592×10^{-3}—7.726×10^{-3} mol dm^{-3}, C_M range 2.469×10^{-3}—2.513×10^{-3} mol dm^{-3}; (1), pH=3.754; (2), pH=4.052; (3), pH=4.660; (4), pH=5.483; (5), pH=5.745; (6), pH=5.875; (7), pH=6.317; (b), C_L range 7.157×10^{-3}—7.219×10^{-3} mol dm^{-3}, C_M range 4.824×10^{-3}—4.866×10^{-3} mol dm^{-3}; (1), pH=3.431; (2), pH=3.783; (3), pH=4.218; (4), pH=4.736] of Cu^{2+}–ahmpe system at 25 °C using the program VISION with the Plotter Calcomp 936.

tion (hyperchromic effect) of the broad spectrum near the IR region and the shift towards smaller wavelengths (hypsochromic effect) of the same band with increasing pH indicates greater complexation, due to the appearance of the hydrolyzed binuclear complex, $[Cu_2(OH)L_2]^+$ (intense green color). When the pH is increased further on from 4.66 to 6.32 (Fig. 3a) small hypochromic and high hypsochromic effects [maximum, 0.218 A at 644 nm(3); 0.182 A at 614 nm(4); 0.175 A at 574 nm(5); Fig. 3a] are observed (change of color from intense green to purple in acid media), while for pH >5.745 a simultaneous increase in the absorption (hyperchromic shift) and a small decrease in the wavelength (hypsochromic effect) [maximum, 0.175 A at 574 nm(5); 0.183 A at 558 nm(6); 0.205 A at 542 nm(7); Fig. 3a] occurs with the formation of the complex $[Cu(OH)L_2]^-$. The color changes from purple to reddish purple. Two distinctive isosbestic points appear at 589 and 483 nm (Fig. 3a). These correspond to an equilibrium between species $[Cu_2(OH)L_2]^+/[CuL_2]$ (each species is present for the 49.0% total copper at pH 5.7, Fig. 2a) and $[CuL_2]/[Cu(OH)L_2]^-$, respectively. It must be noticed that some solutions, several days old, containing Cu^{2+} and ahmpe ligand, both at acid and basic pH values, exhibited a different trend (Fig. 3b). They showed an azure coloring which becomes more intense as the pH increasing (hyperchromic effect), while the maximum shifts slightly towards lower wavelength (hypsochromic shift) [maximum, 0.104 A at 768 nm(1); 0.120 A at 754 nm(2); 0.144 A at 726 nm(3); 0.162 A at 706 nm(4); Fig. 3b]. In order to explain this behavior, we have supposed that the hydroxamate ligand hydrolyzes with the formation

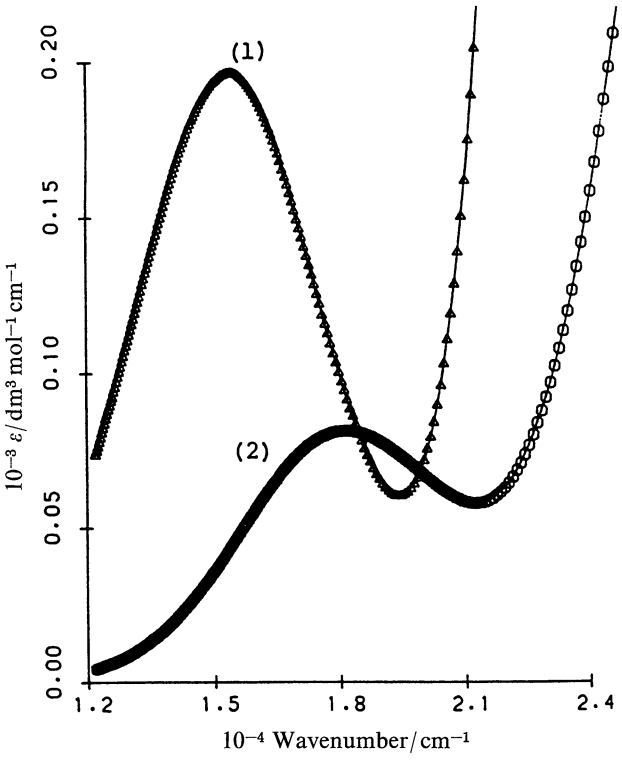

Fig. 4. Plots of molar absorption coefficients (ε) of the two complexed species of Cu^{2+}–ahmpe at 25 °C by program SQUAD: $\varepsilon_{[Cu_2(OH)L_2]^+}$ (1), $\varepsilon_{[CuL_2(H_2O)_2]}$ (2).

of the corresponding amino acid-complexes even in acid solution. In Fig. 4 we have reported molar absorption coefficients (ε) of $[Cu_2(OH)L_2]^+$ and $[CuL_2]$ obtained by use of the program SQUAD in the range 1.2×10^{-4}—2.5×10^{-4} cm^{-1}. The molar absorption coefficients were refined employing 2954 points and obtaining a standard deviation in the absorbance data of 5.9×10^{-2}. By means of the positions of the absorption maxima (Fig. 4), it's possible to check with good precision the ligand-field contribution of ligands about absorbing complexes. According to Billo,[41] the ligand-field contribution of each N (amino) is equal to 4530 cm^{-1}; we can calculate the contribution of each nitrogen of the hydroxamate groups in the $[CuL_2]$ with λ_{max}=18215 cm^{-1} corresponding to: (18215—9060)/2=4577 cm^{-1}. For the hydrolyzed dinuclear complex $[Cu_2(OH)L_2]^+$ with λ_{max}=648 nm, if we suppose coordination of one leucine-hydroxamate residue to each copper ion via the nitrogens of the α-amino and hydroxamate moieties, the global contribution of nitrogen atoms ($-NH_2$ and

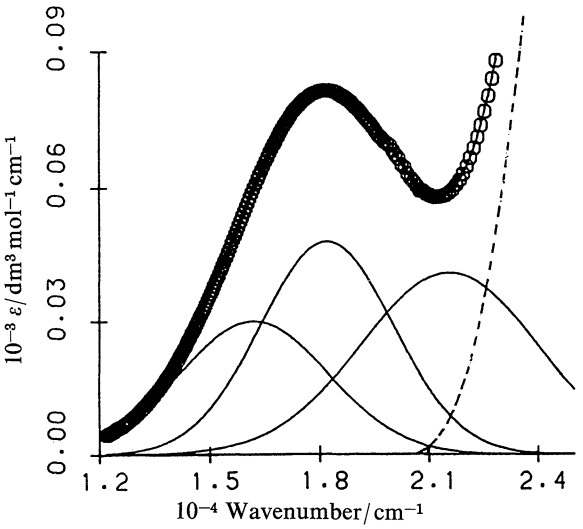

Fig. 5. Absorption spectrum of $[CuL_2(H_2O)_2]$ complex; experimental (symbol) and calculated (line) spectrum; —— components bands, --- unassigned band.

Table 2. Absorption Maxima (nm) and Isosbestic Points (nm) for $[Cu_2(OH)L_2]^+$, $[Cu(OH)L_2]^-$, and $[CuL_2(H_2O)_2]$ Complexes. Parameters (ε/dm^3 mol^{-1} cm^{-1}, ν/cm^{-1}, $\Delta\nu$/cm^{-1}) of the Component Bands Obtained from Gaussian Analysis of the Absorption Spectrum of $[CuL_2(H_2O)_2]$ (L=leucinehydroxamate), f Values Refer to the Oscillator Strengths for the Transitions.[a]

Assignment $[CuL_2(H_2O)_2]$	ε	ν	$\Delta\nu$	f
$^2B_{1g}\longrightarrow{}^2A_{1g}$	29.908	16 199.9	4 773.0	6.5667×10^{-4}
	27.38[b]	16 647.5	3 798.7	4.7844×10^{-4}
	29.29[c]	16 797.8	4 000.1	5.3900×10^{-4}
	34.26[d]	16 800.5	4 001.2	6.3052×10^{-4}
	53.71[e]	16 800.2	4 001.1	9.886×10^{-4}
	33.58[f]	16 799.2	4 147.8	6.404×10^{-4}
	25.734[g]	16 820.4	5 119.6	6.057×10^{-4}
$^2B_{1g}\longrightarrow{}^2B_{2g}$	48.125	18 199.9	4 282.5	9.4807×10^{-4}
	61.00[b]	18 451.4	3 996.9	1.1215×10^{-3}
	54.50[c]	18 492.7	4 378.5	1.0977×10^{-3}
	48.00[d]	18 501.4	4 374.6	9.6595×10^{-4}
	80.93[e]	18 500.2	4 374.9	1.629×10^{-3}
	48.11[f]	18 824.0	4 191.8	9.272×10^{-4}
	53.571[g]	18 382.3	4 861.7	1.197×10^{-3}
$^2B_{1g}\longrightarrow{}^2E_g$	40.985	21 550.1	5 661.5	1.067×10^{-3}
	44.62[b]	21 550.9	5 663.6	1.1625×10^{-3}
	35.26[c]	20 496.3	4 707.9	7.6397×10^{-4}
	36.10[d]	20 500.1	4 705.8	7.8149×10^{-4}
	48.46[e]	20 499.2	4 706.1	1.049×10^{-3}
	29.56[f]	20 517.7	5 066.8	6.855×10^{-4}
	42.472[g]	20 490.9	5 211.2	1.017×10^{-3}

Ligand	$[Cu_2(OH)L_2]^+$	$[Cu(OH)L_2]^-$	$[CuL_2(H_2O)_2]$	Isosbestic point
adhp[e]	653 nm	496 nm	547 nm	594 nm
adhb[d]	651	508	553	595
ahpr[c]	648	518	540	593
ahmpe	648		549	589
aimahp[b]	648	450	536	591
ahbt[h]	647	538	562	602
ahmpe[g]	649		530	595

a) Relative standard deviation (%) or coefficient of variation for Cu^{2+}–ahmpe system=0.23; region of spectrum 12 195—25 000 cm^{-1}. b) Cu^{2+}–aimahp system, Ref. 45. c) Cu^{2+}–ahpr system, Ref. 43. d) Cu^{2+}–adhb system, Ref. 44. e) Cu^{2+}–adhp system, Ref. 46. f) Cu^{2+}–ahpr system, Ref. 39. g) Cu^{2+}–ahmpe system, Ref. 35. h) Cu^{2+}–ahbt system, Ref. 47.

$-NHO^-$) is 9107 cm^{-1}, so the two remaining groups would have to contribute ca. 3162 cm^{-1}. This value agrees well with the predicted contribution of OH^- or H_2O groups of 3010 cm^{-1}. The most important details arising from this work are thermodynamic conclusions, which in some case suggest the structures of the complexes present in aqueous solution. Spectral investigations of structures perceive only those aspects of the structure that are involved in electronic transitions. On the other hand, the spectrophotometric characteristics and the numerical interpretation of the most stable complexes (CuL_2 or FeH_2L_2, $FeHL_2$, and FeL_3) reflect all bond strengths, ring strains, the coordination sphere around the metal ions, and configurations. In order to interpret the $[CuL_2(H_2O)_2]$ spectrum, a careful and detailed Gaussian analysis of the experimental spectrum of $[CuL_2(H_2O)_2]$ (Fig. 5, 201 ε data points in the ν interval of 12200—25000 cm^{-1}) was performed by using the NLIN computer program.[42] This procedure is based on the nonlinear Gauss–Newton least-squares method. In these calculations the parameters of the components bands and related maxima positions were carefully determined. As previously described,[43,44] the assignments and calculated maxima positions of the components bands (Fig. 5, Table 2) allowed D_{4h} symmetry (tetragonally distorted) with four short copper–ligand bonds in one plane (xy) and two longer copper–H_2O bonds lying along the z axis above and below this plane. In this case, the B_{1g} term will be the ground state and three spin-allowed transitions from the $^2B_{1g}$ state to the other doublet states are to be expected.

$[CuL_2(H_2O)_2]$

$$\nu_1 = E(B_{1g} \rightarrow A_{1g}) = -4D_s - 5D_t$$
$$\nu_2 = E(B_{1g} \rightarrow B_{2g}) = 10D_q$$
$$\nu_3 = E(B_{1g} \rightarrow E_g) = 10D_q - 3D_s + 5D_t$$
$$D_q = \nu_2/10 = 1820.0 \text{ cm}^{-1}$$
$$D_s = 1/7[\nu_2 - \nu_1 - \nu_3] = -2792.9 \text{ cm}^{-1}$$
$$D_t = 1/35[4(\nu_3 - \nu_2) - 3\nu_1] = -1005.7 \text{ cm}^{-1}$$

In Table 2 the comparison of the spectrophotometric properties of copper(II)–ahmpe complexes ($[Cu_2(OH)L_2]^+$, $[CuL_2(H_2O)_2]$, and $[Cu(OH)L_2]^-$) with others of amino hydroxamic acids[35,39,43–47] already studied is summarized. From the results obtained, it is possible to verify an excellent agreement between the parameters of the components bands (ε, ν, f, $\Delta\nu$) for the different systems, meaning that a similar behavior (thermodynamic stability, structure, configuration, coordination sphere, etc.) takes place through the $[CuL_2(H_2O)_2]$ complex formation. In particular our results concerning this system are in good agreement with those reported earlier for copper (II)–ahmpe.[35] As regards the compositions and stability constants of the complexes, our results are in fairly good agreement with the above mentioned ones. However, the small differences observed in the parameters D_s and D_t for the different systems means that the energies for a tetragonal distortion, commonly given in terms of the radial parameters, are slightly different for $[CuL_2(H_2O)_2]$. The differences observed in the values D_q and ε could be due to various factors: changes in the metal ligand distance, while the increment in the molar absorption intensity (ε) of the components bands involves a change from centrosymmetric coordination sphere to weakly acentric molecules. Typical titration curves (observed and calculated) for Fe(III)–ahmpe mixtures are shown in Figs. 6a, b. The titration curves obtained on variation of iron and ligand concentration (Figs. 6a, b) were processed in addition to SUPERQUAD program by

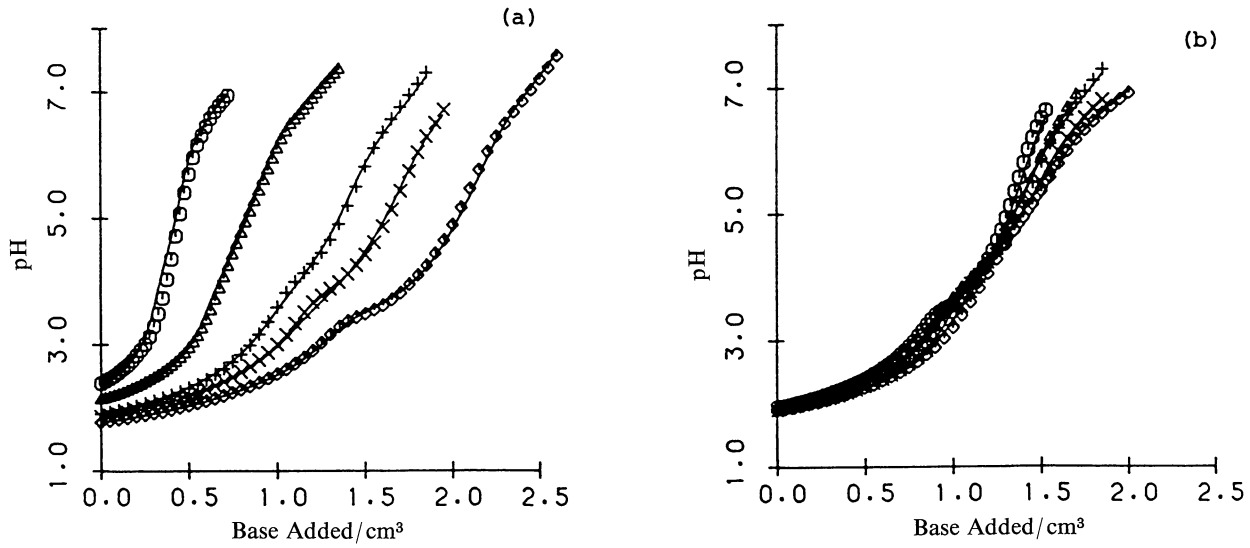

Fig. 6. Experimental and calculated (by SUPERQUAD program) titration curves of pH as a function of volume of KOH added for Fe^{3+}–ahmpe system, V_o=25 cm^3. (a), C_{KOH}=0.46364 mol dm^{-3} [T_L= 0.37732, T_M range 0.03839—0.19628, T_H range 0.81563—1.06633]; (b), C_{KOH}=0.46403 mol dm^{-3}, [T_L range 0.26070—0.59685, T_M=0.12798, T_H range 0.72466—1.39698]. T_L, T_M, and T_H are mmol of ahmpe, iron(III), and hydrogen ion in the titration vessel.

procedures in the FICS method to give $\partial C_H/\partial C_M$ or $\partial C_H/\partial C_L$ respectively, as a function of pH. Finally, the NONLINEAR LS REFINE subprogram of STBLTY[31,32,45,47,48] was applied to select and refine the existing species in the system. From numerous models, the one which yielded the best fit of the titration data (see Figs. 6a, b) is given in Table 1. Our model is only in partial agreement with those given by Brown et al.[17] and El-Ezaby and Hassan[22] for the analogous iron(III)–amino hydroxamate systems. In particular, besides other species of minor importance, the totally deprotonated species $[FeL]^{2+}$ was not found in a quite acid pH range. The relative importance of the various species in each pH range is shown by the typical distribution graph for Fe^{3+}–ahmpe (Fig. 2b). In the presence of Fe^{3+}, the species distribution curves show that complexation begins at low pH values <1.6 for $[Fe(HL)]^{3+}$ species (max. 52.4% total iron at pH 2.0) corresponding to the displacement of one proton. As the pH increases, the proton liberation data shows that complexation proceeds further and at pH 3.3 the predominant species is $[FeH_2L_2]^{3+}$ (74.7%) corresponding to the displacement of two protons. At pH 4.45, the proton displacement value rises to about 3.0 and can be attributed to the formation of the $[FeHL_2]^{2+}$ (48.3%) species when the hydroxamate moiety is about 59.8% ionized. As the pH increases further, the major species present are: $[FeH_2L_3]^{2+}$ (max. 40.9% at pH 5.85), $[FeHL_3]^{+}$ (max. 47.8% at pH 7.05), and $[FeL_3]$ (max. 53.4% at pH 8.0). In these last species three hydroxamate groups can satisfy the octahedral configuration around iron (III), but the $[FeL_3]$ complex formation can be reached only at very high free ligand concentration. Additionally, the formation of protonated, deprotonated and/or mixed hydroxo complexes can be assumed. The spectrophotometric study was carried out on a series of solutions containing ahmpe and iron ions, with concentrations and pH values selected from those employed in the potentiometric titrations. The visible spectra of the Fe^{3+}–ahmpe system as a function of pH are shown in Fig. 7. When the pH is increased from 1.784 to 3.060 [maximum, 0.605 A at 480 nm(1); 0.663 A at 480 nm(2); 0.738 A at 474 nm(3); 0.858 A at 472 nm(4); 1.059 A at 464 nm(5); Fig. 7] small hypsochromic and high hyperchromic effects are observed (intense reddish brown), indicating that complexation at this pH interval presumably gives $[FeHL]^{3+}$, $[FeH_2L_2]^{3+}$, and $[FeHL_2]^{2+}$ (Fig. 2b). A maximum at 464 nm [curve (5), Fig. 7] is reached at pH 3.060, which corresponds to the maximum in the concentration (71.0%) of the protonated complex, $[FeL_2L_2]^{3+}$.

As the pH increases further on a decrease in the wavelength and an increase in the absorption occurs with a maximum at 448 nm [curve (7), Fig. 7]. The color of the solution changes from wine red [intense reddish brown, pH 1.78 to 3.93] to orange red at pH ca. 4.5 and remains this color up to pH 8.0. Componentization of the visible spectra (300—700 nm) data deduced by refinement procedure with program SQUAD indicates at least six colored species are present between 1.784—7.900 pH values. The 13 spectra, each containing 201 absorbance values between 300 and 700 nm, could be presented as linear combinations of six "components"

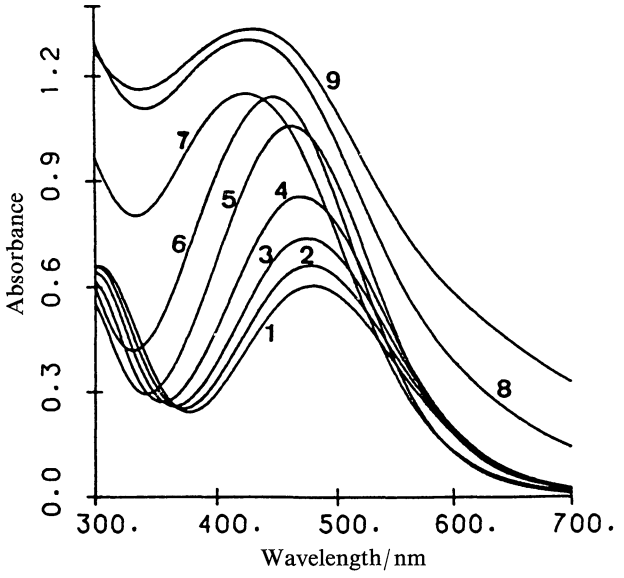

Fig. 7. Plots of experimental data versus wavelength for solutions [C_L range 1.517×10^{-2}—1.647×10^{-2} mol dm^{-3}, C_M range 5.659×10^{-3}—6.143×10^{-3} mol dm^{-3}; (1), pH=1.784; (2), pH=1.930; (3), pH=2.139; (4), pH=2.455; (5), pH=3.060; (6), pH=3.931; (7), pH=5.233; (8), pH=6.592; (9), pH=7.442] of Fe^{3+}–ahmpe system at 25 °C using the program VISION with the Plotter Calcomp 936.

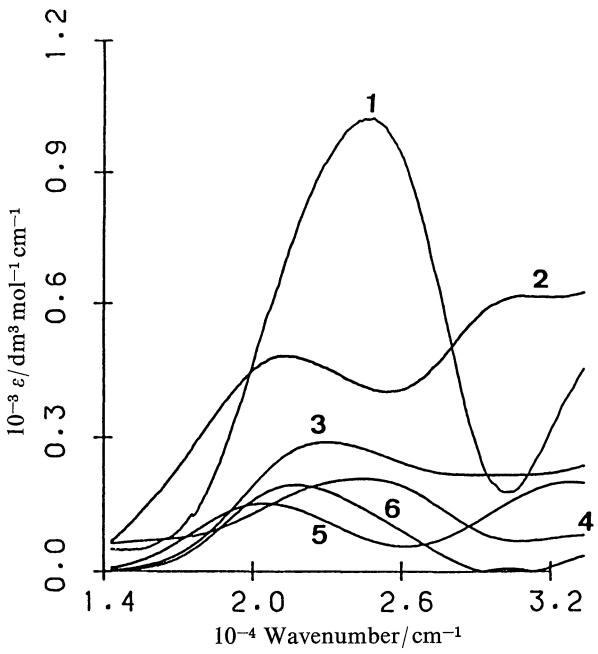

Fig. 8. Plots of molar absorption coefficients (ε) of the six complexed species of Fe^{3+}–ahmpe system: (1) $\varepsilon_{Fe_2(OH)L_3}$, (2) ε_{FeHL_3}, (3) ε_{FeHL_2}, (4) ε_{FeL_3}, (5) $\varepsilon_{FeH_2L_2}$, (6) ε_{FeHL}.

(or molar extinction coefficients, Fig. 8) spectra within standard deviation in absorbance of 0.0201. The least-squares modeling of the spectra included a very small contribution from absorption by Fe^{3+} and its hydrolyzed species (determined from the absorbance of dilute $Fe(NO_3)_3$ solutions at different pH values) in addition to major contributions from six Fe^{3+}–ahmpe complexes. Since iron(III) is a typical hard ion, we presume the coordination of O,O atoms of hydroxamate moiety of ahmpe. Accordingly, the protonated $[FeHL]^{3+}$ $[FeH_2L_2]^{3+}$, $[FeHL_2]^{2+}$, $[FeH_2L_3]^{2+}$, and $[FeHL_3]^{+}$ complexes contain the amino group in its protonated form. This assumption is supported by the spectrophotometric results (see Fig. 7) and those recorded for iron(III)–hydroxamate systems.[45,49–51]

Grateful acknowledgement is made to the Ministero della Pubblica Istruzione (Rome) and National Research Council of Italy (C.N.R.) for generous grants. I am greatly indebted to Professors P. Gans, A. Sabatini, and A. Vacca for their generous support of the program SUPERQUAD.

References

1) J. O. Baker, S. H. Wilkes, M. E. Bayliss, and J. M. Prescott, *Biochemistry,* **22**, 2098 (1983).
2) S. H. Wilkes and J. M. Prescott, *J. Biol. Chem.,* **258**, 13517 (1983).
3) M.-A. Coletti-Previero, A. Crastes de Paulet, H. Mattras, and A. Previero, *Biochem. Biophys. Res. Commun.,* **107**, 465 (1982).
4) J. B. Summers, H. Mazdijasni, J. H. Holms, J. D. Ratajczyk, R. D. Dyer, and G. W. Carter, *J. Med. Chem.,* **30**, 574 (1987).
5) E. J. Corey, J. R. Cashman, S. R. Kantner, and S. W. Wright, *J. Am. Chem. Soc.,* **106**, 1503 (1984).
6) W. M. Moore and C. A. Spilburg, *Biochem. Biophys. Res. Commun.,* **136**, 390 (1986).
7) S. Blumberg, Z. Vogel, and M. Altstein, *Life Sci.,* **28**, 301 (1981).
8) R. Boubouton, G. Waksman, J. Devin, N. C. Fournie-Zaluski, and B. P. Roques, *Life Sci.,* **35**, 1023 (1984).
9) N. Nishino and J. C. Powers, *Biochem. Biophys. Res. Commun.,* **17**, 2846 (1978).
10) R. B. Harris, P. D. M. Strong, and I. B. Wilson, *Biochem. Biophys. Res. Commun.,* **116**, 394 (1983).
11) E. Farkas and I. Kiss, *J. Chem. Soc., Dalton Trans.,* **1990**, 749.
12) C. A. Chang, V. C. Sekhar, B. S. Garg, F. S. Guziec, and T. Carrera Russo, *Inorg. Chim. Acta,* **135**, 11 (1987).
13) W. R. Harris, C. J. Carrano, S. R. Cooper, S. R. Sofen, A. E. Avdeef, J. V. Mc Ardle, and K. N. Raymond, *J. Am. Chem. Soc.,* **101**, 6097 (1979).
14) Chiu Yuen Ng, S. J. Rodgers, and K. N. Raymond, *Inorg. Chem.,* **28**, 2062 (1989).
15) D. A. Brown, R. Geraty, J. D. Glennon, and N. N. Choileain, *Inorg. Chem.,* **25**, 3792 (1986).
16) A. Shanzer, J. Libman, R. Lazar, and Y. Tor, *Pure Appl. Chem.,* **61**, 1529 (1989).
17) D. A. Brown, M. V. Chidambaram, and J. D. Glennon, *Inorg. Chem.,* **19**, 3260 (1980).
18) K. N. Raymond and T. M. Garrett, *Pure Appl. Chem.,* **60**, 1807 (1988).
19) Y. K. Agrawal and G. D. Mehd, *Int. J. Environ. Anal. Chem.,* **10**, 183 (1981).
20) D. C. Bhura and S. B. Tandon, *Anal. Chim. Acta,* **53**, 379 (1971).
21) R. M. Cassidy and D. E. Ryan, *Can. J. Chem.,* **46**, 327 (1968).
22) M. S. El-Ezaby and M. M. Hassan, *Polyhedron,* **4**, 429 (1985).
23) M. S. El-Ezaby, H. M. Marafie, and H. M. Abu-Soud, *Polyhedron,* **5**, 973 (1986).
24) N. E Dixon, R. L. Blakely, and B. Zerner, *Can. J. Biochem.,* **58**, 1323 (1980).
25) G. Gran, *Analyst (London),* **77**, 661 (1952).
26) H. S. Harris and R. S. Tobias, *Inorg. Chem.,* **8**, 2259 (1969).
27) E. Leporati, *J. Chem. Soc., Dalton Trans.,* **1985**, 1605.
28) E. Leporati, *J. Chem. Soc., Dalton Trans.,* **1986**, 199.
29) R. S. Tobias and M. Yasuda, *Inorg. Chem.,* **2**, 1307 (1963).
30) P. Gans, A. Sabatini, and A. Vacca, *J. Chem. Soc., Dalton Trans.,* **1985**, 1195.
31) B. Sarkar and T. P. A. Kruck, *Can. J. Chem.,* **51**, 3541 (1973).
32) R. Osterberg, *Acta Chem. Scand.,* **14**, 471 (1960).
33) N. Ingri, W. Kakalowicz, L. G. Sillén, and B. Warnqvist, *Talanta,* **14**, 1261 (1967).
34) D. J. Leggett and W. A. E. Mc Bryde, *Anal. Chem.,* **47**, 1065 (1975).
35) B. Kurzak, K. Kurzak, and J. Jezierska, *Inorg. Chim. Acta,* **130**, 189 (1987).
36) A. Gergely, I. Sovago, I. Nagypal, and R. Kiraly, *Inorg. Chim. Acta,* **6**, 435 (1972).
37) G. H. Khoe, P. L. Brown, R. N. Sylva, and R. G. Robins, *J. Chem. Soc., Dalton Trans.,* **1986**, 1901.
38) C. F. Baes, Jr. and R. E. Mesmer, "The Hydrolysis of Cations," Wiley Interscience, New York (1976).
39) B. Kurzak, K. Kurzak, and J. Jezierska, *Inorg. Chim. Acta,* **125**, 77 (1986).
40) E. B. Paniago and S. Carvalho, *Inorg. Chim. Acta,* **92**, 253 (1984).
41) E. J. Billo, *Inorg. Nucl. Chem. Lett.,* **10**, 613 (1974).
42) "SAS User's Guide: Statistics, Version 5," SAS Institute Inc., Cary, Nc. (1985), p. 576.
43) E. Leporati, *J. Chem. Soc., Dalton Trans.,* **1989**, 1299.
44) E. Leporati, *Inorg. Chem.,* **28**, 3752 (1989).
45) E. Leporati and G. Nardi, *Gazz. Chim. Ital.,* **121**, 147 (1991).
46) E. Leporati, *Gazz. Chim. Ital.,* **119**, 183 (1989).
47) E. Leporati, *J. Chem. Res. (S),* **1990**, 14.
48) D. J. Leggett, "Computational Methods for the Determination of Formation Constants," Plenum Press: New York and London (1987), p. 355.
49) E. Farkas, J. Szoke, T. Kiss, K. Kozlowski, and W. Bal, *J. Chem. Soc., Dalton Trans.,* **1989**, 2247.
50) J. Neilands, *Struct. Bonding (Berlin),* **1**, 59 (1966).
51) D. A. Brown, R. Mageswaran, *Inorg. Chim. Acta,* **161**, 267 (1989).